Journal of Magnetism and Magnetic Materials 477 (2019) 156–161

Contents lists available at ScienceDirect

Journal of Magnetism and Magnetic Materials

journal homepage: www.elsevier.com/locate/jmmm

Research articles

Effect of Co addition and annealing conditions on the magnetic properties of nanocrystalline FeCoSiBPCu ribbons

Bao-wen Miao[a], Qiang Luo[a,*], Chun-tao Chang[b,c], Tao Liu[b,c], Yan Zhang[d,*], Jun Shen[a,d,e]

[a] School of Materials Science and Engineering, Tongji University, 4800 Caoan Road, Shanghai 201804, China
[b] Key Laboratory of Magnetic Materials and Devices, Ningbo Institute of Materials Technology and Engineering, Chinese Academy of Sciences, Ningbo, Zhejiang 315201, China
[c] Zhejiang Province Key Laboratory of Magnetic Materials and ApplicationTechnology, Ningbo Institute of Materials Technology and Engineering, Chinese Academy of Sciences, Ningbo 315201, China
[d] Institute for Materials Research, Tohoku University, Sendai 980-8577, Japan
[e] College of Mechatronics and Control Engineering, Shenzhen University, Shenzhen 518060, China

ARTICLE INFO

Keywords:
Soft magnetic property
Nanocrystalline alloy
Microstructure
Coercivity
Core loss

ABSTRACT

We report the effect of substituting Co for a metalloid element on the glass formation, thermal properties, and magnetic behaviors of $Fe_{80}Co_xB_{14-x}Si_2P_3Cu_1$ (x = 0, 2, 4, 6) alloy ribbons. The addition of Co decreased the thermal stability of the alloy against crystallization and expanded the heat treatment temperature region of this alloy family. $Fe_{80}Co_4B_{10}Si_2P_3Cu_1$ alloy, which was annealed under optimal conditions, exhibited good soft magnetic performance that was characterized by a high saturation magnetic flux density of 1.84 T, a high effective magnetic conductivity of 12,601 at 1000 Hz, a low coercivity of 5.3 A/m, and a low core loss of 62 W/kg at 1000 Hz and 1.5 T.

1. Introduction

Requirements for minimizing energy loss have become increasingly stringent as critical global environment problems continue to intensify. Soft magnetic materials with high saturation magnetization (M_s) (or magnetic flux density [B_s]), high effective magnetic conductivity (μ_e), low magnetic core loss (W), and low coercivity (H_c) must be designed to reduce energy losses in magnetic applications [1–15]. Si steel has been widely used as a soft magnetic material because it satisfies most soft magnetic property requirements, such as high B_s. Nevertheless, it presents several considerable shortcomings, including high W and large H_c. Three alloy family systems with excellent soft magnetic properties have been developed to meet environmental requirements and reduce production costs. These alloy families are FINEMET [16], NANOPERM [17], and HITPERM [18]. FINEMET alloys have good glass-forming ability [1,19–20]. Nevertheless, the M_s of FINEMET alloys is lower than that of Si steel. This characteristic limits the extensive commercial applications of FINEMENT alloys. HITPERM and NANOPERM alloys have high M_s but mediocre soft magnetic properties [11,12]. These alloys have low Fe contents because they contain numerous metal/metalloid elements that account for their uniform amorphous/nanocrystalline microstructures [21–25]. The development of Fe-based soft magnetic alloys with Fe contents exceeding 80% is important for practical applications [24–32]. Fe-based alloys with excellent soft magnetic performance can be obtained through the uniform precipitation of nanoscale bcc Fe (α-Fe) grains [25]. The B_s of binary Fe–Co alloys is higher than that of pure Fe [4,22,33–35] and can be enhanced when Fe–Co grains, instead of bcc Fe, precipitate in the alloys. Co-based amorphous alloys with the magnetic permeability of 1,000,000 have become popular, and the addition of nonmagnetic glass formers, such as Si and B elements, can reduce the B_s of amorphous alloy systems. For example, the addition of Si reduces the M_s of Co-augmented FINEMET alloys by inducing the preferential formation of the $(Fe, Co)_3Si$ phase [23]. This result indicates that the appropriate replacement of metalloid elements with Co may improve the magnetic properties of Fe-based alloys. The addition of Co may increase the cost of alloys but may also improve soft magnetic performance. Thus, its effect on the local structure, crystallization, and magnetic properties of amorphous and nanocrystalline alloys must be explored. The beneficial effect of Co addition on the magnetic behavior of amorphous and (nano)crystalline alloys has already been verified in many systems [22,24,25,28,30–32,35]. In addition, the addition of a small amount of Co can facilitate the production of wide ribbons, which are specially required in some commercial applications, such as transformers and

* Corresponding authors.
E-mail addresses: zf17lq@sina.com (Q. Luo), zy-jp@imr.tohoku.ac.jp (Y. Zhang).

https://doi.org/10.1016/j.jmmm.2019.01.052
Received 20 May 2018; Received in revised form 12 January 2019; Accepted 14 January 2019
Available online 16 January 2019
0304-8853/

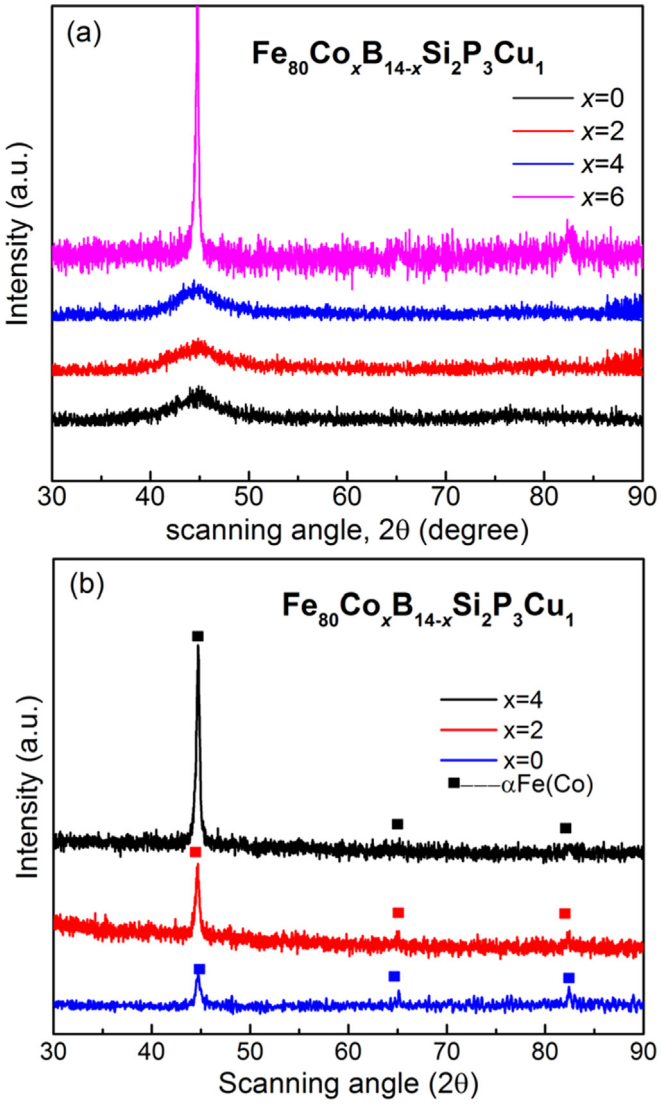

Fig. 1. XRD patterns of various $Fe_{80}Co_xB_{14-x}Si_2P_3Cu_1$ (a) as-spun ribbons and (b) annealed ribbons.

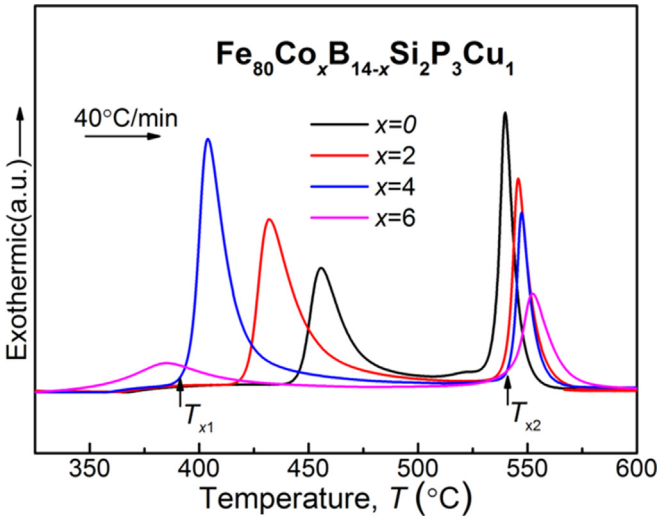

Fig. 2. DSC curves of the as-spun amorphous FeCoBSiPCu alloy ribbons.

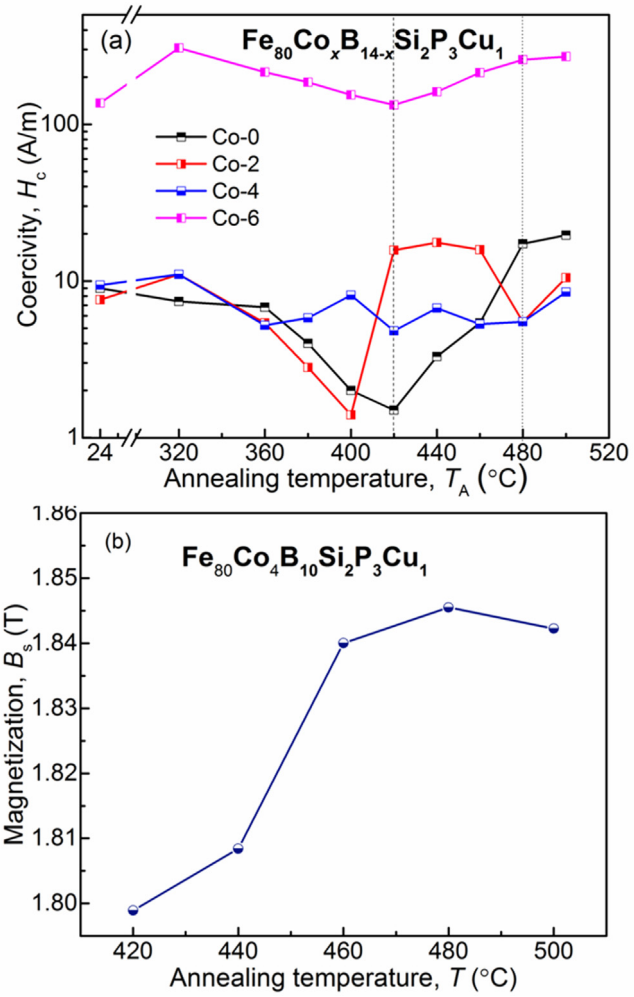

Fig. 3. (a) Dependence of H_c on the annealing temperature (T_a) for the $Fe_{80}Co_xB_{14-x}Si_2P_3Cu_1$ alloy ribbons; (b) Dependence of B_s on the annealing temperature (T_a) for the $Fe_{80}Co_4B_{10}.Si_2P_3Cu_1$ alloy.

motors. [33].

The $Fe_{80}Si_2B_{14}P_3Cu_1$ alloy system has low Si content and high B content. Given these characteristics, the soft magnetic performance of this system could be improved by replacing B with Co. In this study, we explored the glass formation ability, thermal stability, and magnetic behavior of the $Fe_{80}Co_xB_{14-x}Si_2P_3Cu_1$ (x = 0, 2, 4, 6) alloy system and elucidated the soft magnetic performances of $Fe_{80}Co_4B_{10}Si_2P_3Cu_1$ alloy. The addition of small amounts of Co remarkably affected glass formation, crystallization, and magnetic behavior of the alloy systems. Co content was limited to 6% in consideration of fabrication costs.

2. Experiment

Alloy ingots with the nominal compositions of $Fe_{80}Co_xB_{14-x}Si_2P_3Cu_1$ were dissolved through the induction melting of a mixture of pure Fe (99.99 mass%), Fe_3P (99.9 mass%), B (99.5 mass %), Co (99.999 mass%), Si (99.9 mass%), and Cu (99.9 mass%) under an Ar atmosphere. Ribbons with thicknesses of ~22 μm were then prepared from the alloy ingots via the melt spinning technique. All samples were fabricated under the same conditions. The microstructures of the as-spun and annealed ribbons were checked via X-ray diffraction under Cu Kα radiation and transmission electron microscopy (TEM). The thermal stability and crystallization temperature (T_x) of the as-spun samples were determined through differential scanning calorimetry (DSC) with the heating rate of 40 °C/min under Ar flow.

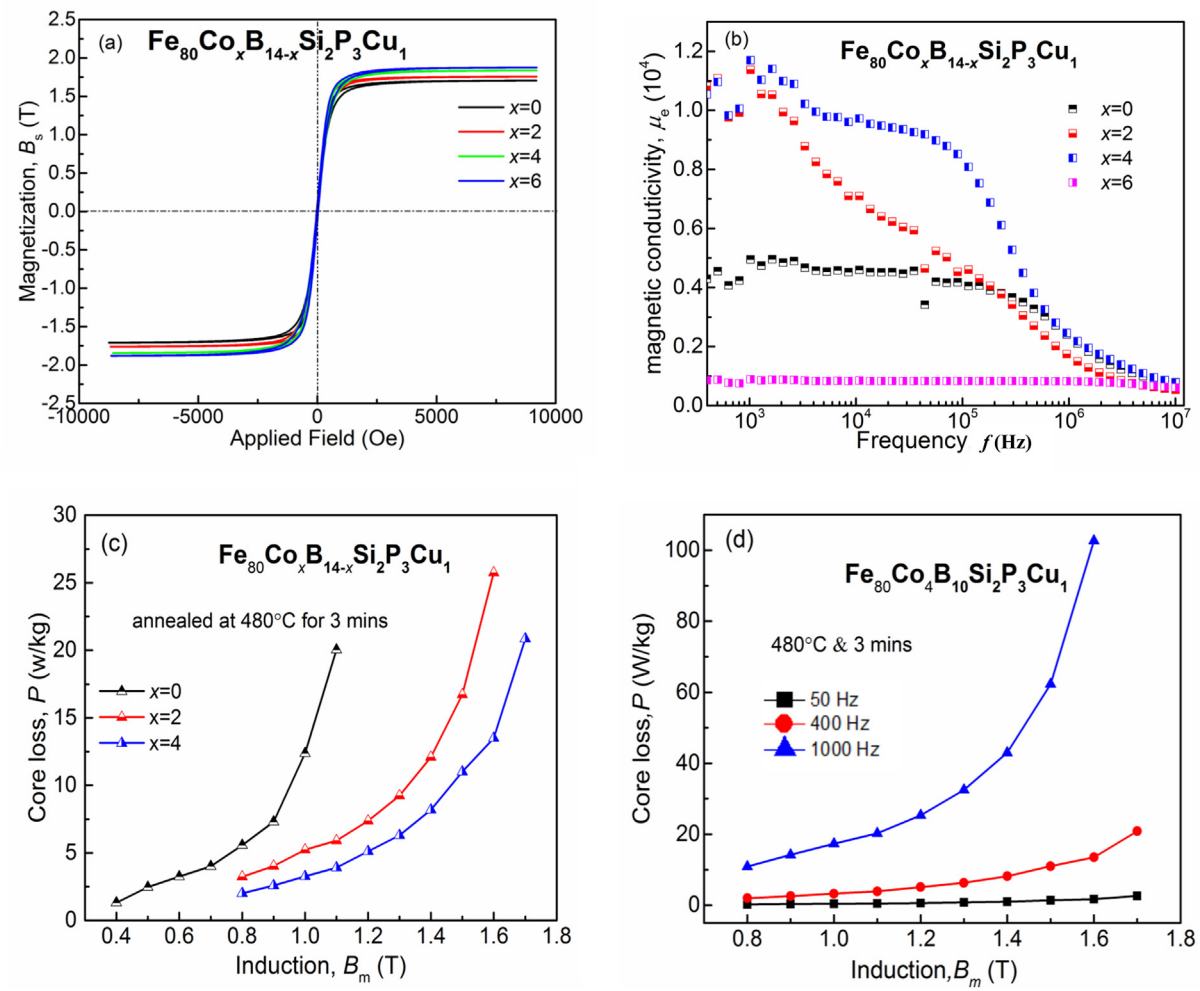

Fig. 4. (a) Hysteresis curves of annealed ribbons of $Fe_{80}Co_xB_{14-x}Si_2P_3Cu_1$ alloy; (b) Dependence of magnetic conductivity on frequency for the $Fe_{80}Co_xB_{14-x}Si_2P_3Cu_1$ alloy ribbons; (c) Dependence of magnetic core loss (W) on the induction for the $Fe_{80}Co_xB_{14-x}Si_2P_3Cu_1$ alloy ribbons at 50 Hz. (d) Dependence of magnetic core loss (P) on the induction for the $Fe_{80}Co_4B_{10-}Si_2P_3Cu_1$ alloy ribbon at 50 Hz, 400 Hz, 1000 Hz.

The as-spun alloys were nanocrystallized through annealing under various temperatures in a vacuum in zero magnetic field for different durations. Magnetic behaviors, specifically, B_s and M_s, were quantified with a vibrating sample magnetometer under a field strength of 15,000 Oe. A DC B-H loop tracer was used to determine H_c, and an ac B-H analyzer was used to determine W. Magnetic conductivity was obtained at different frequencies by an impedance analyzer.

3. Results and discussion

The X-ray diffraction spectra of $Fe_{80}Co_xB_{14-x}Si_2P_3Cu_1$ (x = 0, 2, 4, 6) alloy ribbons with different Co contents are presented in Fig. 1. The free surfaces of the samples were examined. The absence of a discernible diffraction peak from the XRD patterns of the alloy ribbons with Co contents of 0–4 at.% indicates that all these alloys were fully amorphous. Nevertheless, a sharp diffraction peak appeared in the spectra of the alloy ribbons with Co contents of 6 at.%. The presence of this peak shows that the alloy ribbons had partly crystallized. The partially crystallized ribbon will not be considered for further magnetic studies because it exhibited a high H_c. The XRD and DSC results presented in Figs. 1 and 2 revealed that the partial substitution of B with Co impaired the glass forming ability of the present alloy system because excessive Co content promoted the formation of the α-(Fe, Co) phase in the undercooled liquid. This effect was particularly pronounced when Co content reached 6%. By contrast, the alloy system with the Co content of less than 6% remained in an amorphous state.

Fig. 2 presents the thermal properties of the as-spun $Fe_{80}Co_xB_{14-x}Si_2P_3Cu_1$ (x = 0, 2, 4, 6) alloy ribbons. All of the samples underwent two-stage crystallization processes [24]. In the first stage of crystallization, the amorphous phase partially transformed into the nanocrystalline α-(Fe, Co) phase; in the second stage, the remaining amorphous phases crystallized [24–27]. T_{x1} and T_{x2} are the onset temperatures of the first and second crystallization events, respectively. T_{x1} and T_{x2} decreased and increased, respectively, as Co concentration increased. Therefore, the addition of Co expanded the temperature interval ΔT_x ($\Delta T_x = T_{x2} - T_{x1}$). This effect may enhance the room- and high-temperature magnetic performance of the alloys by improving the control of nanocrystalline formation in the amorphous matrix during annealing [28]. An alloy should contain high concentrations of single-phase nanocrystals that are uniformly embedded in an amorphous matrix to exhibit good soft magnetic properties [25,26].

The optimal annealing conditions were identified by heat-treating the as-spun alloys in a vacuum under different annealing temperatures (T_a) between T_{x1} and T_{x2}. Fig. 3(a) and (b) show the annealing temperature-dependent behaviors of H_c and B_s, respectively. The relationship between the T_a and H_c of the annealed ribbons with different compositions is shown in Fig. 3(a). The H_c of all ribbons first decreased with T_a up to $T_{x1} - 40$ °C and then increased gradually when T_a exceeded $T_{x1} - 40$ °C. The H_c of the ribbons decreased at low T_a (below T_{x1}) owing to the release of internal stress. The precipitation of α-(Fe,

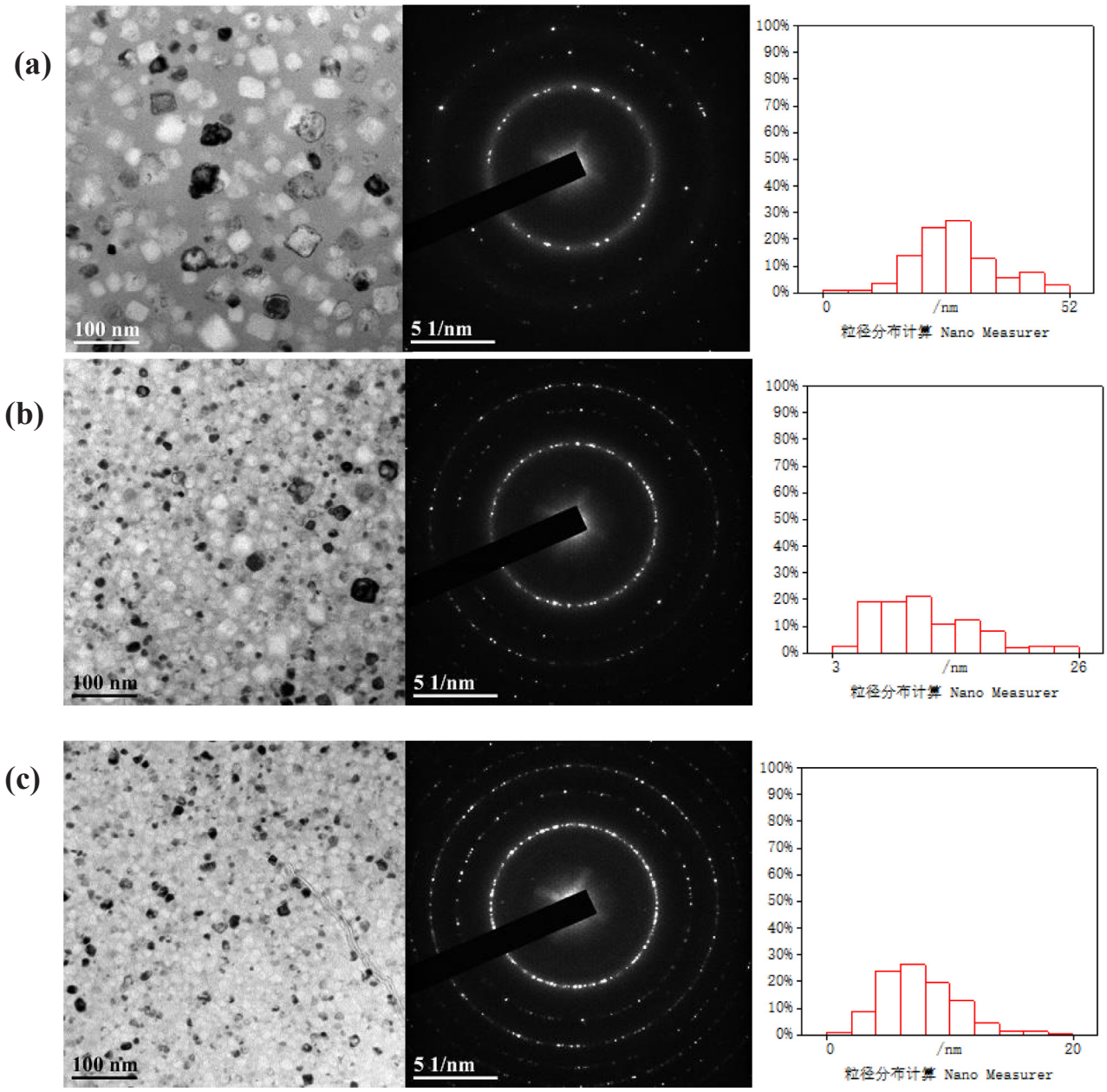

Fig. 5. TEM images of ribbons (a) $Fe_{80}B_{14}Si_2P_3Cu_1$; (b) $Fe_{80}Co_2B_{12}Si_2P_3Cu_1$; (c) $Fe_{80}Co_4Si_{2-}P_3Cu_1$ annealed at optimum annealing conditions, respectively.

Co) grains from the amorphous matrix as T_a approached T_{x1} increased H_c [24]. Further increasing the annealing temperatures to slightly above T_{x1} resulted in the formation of numerous fine α-(Fe, Co) grains and thus facilitated exchange coupling between grains [24,36]. However, the formation of other compounds will drastically degrade the soft magnetic properties of samples annealed at temperatures that were considerably higher than T_{x1}. Therefore, as inferred from the DSC results, the optimum annealing temperature region ranged from 420 °C to 480 °C, and the $Fe_{80}Co_xB_{14-x}Si_2P_3Cu_1$ (x = 0, 2, 4, 6) alloys presented the lowest H_c of 5.3 A/m after annealing. The x = 6 sample consistently provided an extremely large H_c (above 200 A/m) given that it contained large crystals. Although nanocrystalline alloys with H_c above 100 A/m can exhibit high B_s, they are not promising for applications that require extremely low W. The present alloy system showed good comprehensive soft magnetic performances despite its fair H_c of −5.3 A/m [16,34], as discussed below.

The relationship between annealing temperature and *Bs* is shown in Fig. 3(b). The $Fe_{80}Co_4B_{10}Si_2P_3Cu_1$ alloy was used as an example. B_s increased as annealing temperature increased when T_a was lower than 480 °C and began to decrease when T_a exceeded 480 °C. Experimental results showed that the optimal annealing treatment condition for obtaining the best soft magnetic performance was 480 °C for 3 min.

The Co-dependence of the B_s, μ_e, W, and H_c of the alloys annealed under the optimal heat treatment conditions is discussed in the following section. B_s can be determined from the B–H curves shown in Fig. 4(a). $Fe_{80}Co_4B_{10}Si_2P_3Cu_1$ and $Fe_{80}B_{14}Si_2P_3Cu_1$ exhibited the maximum and minimum B_s values of 1.84 and 1.70 T, respectively. These results can be attributed to the formation of fine nanocrystals in the amorphous matrix in the presence of small amounts of Co. The complexity of the nanocrystallization mechanism of Fe–Si–B–P–Cu alloys may be attributed to pre-existing fine α-Fe nuclei in the as-quenched alloys. Therefore, pre-existing and newly created nuclei must grow together during annealing to yield a uniform nanocrystalline grain structure that confers good soft magnetic performance to the final alloy system. XRD and magnetic results revealed that the addition of low Co amounts promoted fine nanocrystalline formation. Nevertheless, the

presence of large crystals hindered the as-quenched x = 6 sample from developing fine and uniform nanocrystals during annealing. Similar to that in the case of ball-milled Fe–Co alloys, the increase in the B_s of the Fe–Si–B–P–Cu alloys after Co addition may be attributed to α-(Fe, Co) solid solution formation [4,22]. The change in B_s with Co content can be ascribed to the differences among the grain sizes of α-(Fe, Co) as will be discussed further below. The nanocrystalline alloy with the Co concentration of −4 at.% presented the lowest H_c (−5.3 A/m) and highest *Bs* (−1.84 T). It is possible to obtain a fine nanocrystalline structure with α-(Fe, Co) phase in as-quenched alloys with higher concentration of Co to get higher B_s.

The variation in the μ_e of the $Fe_{80}Co_xB_{14-x}Si_2P_3Cu_1$ (x = 0, 2, 4, 6) ribbons with frequency is illustrated in Fig. 4 (b). The μ_e of all ribbons, but not that of $Fe_{80}Co_6B_8Si_2P_3Cu_1$, increased as Co content increased because the grain size of α-(Fe, Co) decreased with increasing Co content. Permeability is expected to vary roughly with grain size as $\mu_e \propto 1/D^6$. Magnetic conductivity at 1000 Hz is an important index of the soft magnetic property of a nanocrystalline alloy. The alloy with −4 at.% Co content obtained the highest μ_e of −12,601 and that without Co content obtained the low μ_e of 4949. The μ_e of $Fe_{80}Co_4B_{10}Si_2P_3Cu_1$ alloy remained high even under high frequency.

Fig. 4(c) shows the variation in the *W* of $Fe_{80}Co_xB_{14-x}Si_2P_3Cu_1$ (x = 0, 2, 4) ribbons at 50 Hz as a function of Co content. Substituting Co with B accelerated the magnetic core loss of the ribbons. The x = 4 sample showed the lowest *W* over a wide range of magnetic induction. This characteristic is related to its small nanograin size and low H_c. In addition to B_s, *W* is the most important property considered in the high-frequency application of soft magnetic alloys as motors and transformers. The *W* of $Fe_{80}Co_4B_{10}Si_2P_3Cu_1$ alloy was measured at frequencies of 50, 400, and 1000 Hz and different magnetic inductions (B_m) (Fig. 4[d]). The $Fe_{80}Co_4B_{10}Si_2P_3Cu_1$ alloy exhibited a low *W* of 60 *W*/kg at the high B_m of −1.5 T and frequency of −1000 Hz. These characteristics are important for minimizing energy loss in many magnetic applications.

The microstructures of the alloys were analyzed via XRD and TEM to elucidate the effect of Co concentration on magnetic behaviors. The results for alloys containing −0% to 4% Co are shown in this section. Fig. 5(a)–(c) provide the TEM images of the annealed $Fe_{80}B_{14}Si_2P_3Cu_1$, $Fe_{80}Co_2B_{12}Si_2P_3Cu_1$, and $Fe_{80}Co_4B_{10}Si_2P_3Cu_1$ samples, respectively. Nanocrystals precipitated in the amorphous matrix, and the average grain size of nanocrystals decreased as Co content increased. The SAED patterns (inset in Fig. 5) of the alloys also indicate that α-(Fe, Co) nanocrystals oriented in the annealed samples randomly. Small α-(Fe, Co) grain sizes favor low H_c [28,29]. The TEM images were subjected to statistical analysis to obtain grain size information. More than 100 spots were analyzed for the determination of mean grain size. The mean grain sizes of $Fe_{80}B_{14}Si_2P_3Cu_1$, $Fe_{80}Co_2B_{12}Si_2P_3Cu_1$, and $Fe_{80}Co_4B_{10}Si_2P_3Cu_1$ were 27.74, 11.75, and 7.61 nm, respectively. These results illustrate that grain size tended to decrease as Co content increased. H_c was expected to vary with grain size as $H_c \propto D^6$. Therefore, the TEM results provide evidence that the development of a uniform nanocrystalline structure with small bcc Fe(-Co) grain sizes and high Co concentration is conducive for reducing H_c. However, the precipitation of large crystals in the x = 6 alloy implies that an upper limit exists for the simultaneous achievement of high B_s and low H_c by the Fe–Co–-Si–B–P–Cu alloy systems.

4. Conclusions

The effects of substituting B with Co on the structure, thermal behavior, and magnetic performances of $Fe_{80}Co_xB_{14-x}Si_2P_3Cu_1$ (x = 0, 2, 4, 6) alloys were investigated. XRD measurements revealed that most of the as-spun alloys contained an amorphous phase. The $Fe_{80}Co_6B_8Si_2P_3Cu_1$ ribbon exhibited a composite structure that was characterized by crystalline phases embedded in an amorphous matrix. Replacing B with Co in the present alloy system reduced the thermal stability of the amorphous phase against crystallization but expanded the temperature range for heat treatment, favored the precipitation of α-(Fe, Co), and inhibited the precipitation of other compounds. These effects improved the soft magnetic performance of the alloy systems. The outstanding soft magnetic properties exhibited by the alloy systems when annealed under optimal conditions may be attributed to the formation of a uniform fine α-(Fe,Co) phase. The nanocrystalline $Fe_{80}Co_4B_{10}Si_2P_3Cu_1$ alloy presented a high B_s of 1.84 T, low H_c of 5.3 A/m, high μ_e of 12,601 at 1000 Hz, and low *W* of 62 W/kg at 1000 Hz and 1.5 T. These results indicated that the introduction of a small amount of Co enhanced soft magnetic performance by effectively inducing the uniform nanocrystallization of α-(Fe, Co) and averaging out magnetic anisotropy.

Acknowledgments

This work is supported by the National Key Research and Development Plan of China (Grant No. 2016YFB0300502), the National Science Foundation of China (Grant Nos. 51371127 and 51601130) and the Fundamental Research Funds for the Central Universities (No. 22120180070).

References

[1] Y. Yoshizawa, S. Oguma, K. Yamauchi, New Fe-based soft magnetic alloys composed of ultrafine grain structure, J. Appl. Phys. 64 (1988) 6044–6046.
[2] K. Suzuki, N. Kataoka, A. Inoue, A. Makino, T. Masumoto, High saturation magnetization and soft magnetic properties of bcc Fe-Zr-B alloys ultrafine grain structure, Mater. Trans., JIM 31 (1990) 743–746.
[3] K. Suzuki, A. Makino, A. Inoue, T. Masumoto, Soft magnetic properties of nanocrystalline bcc Fe-Zr-B and Fe-M-B-Cu (M = transition metal) alloys with high saturation magnetization (invited), J. Appl. Phys. 70 (1991) 6232–6237.
[4] C. Kuhrt, L. Schultz, Formation and magnetic properties of nanocrystalline mechanically alloyed Fe-Co, J. Appl. Phys. 71 (1992) 1896–1900.
[5] A. Inoue, Y. Shinohara, J.S. Gook, Thermal and magnetic properties of bulk Fe-based glassy alloys prepared by copper mold casting, Mater. Trans., JIM 36 (1995) 1427–1433.
[6] L. Pascual, C. Gomez-Polo, P. Marin, M. Vazquez, H.A. Davies, Magnetic hardening in nanocrystalline FeCoSiBCuNb alloy, J. Magn. Magn. Mater. 203 (1999) 79–81.
[7] M. Ohta, Y. Yoshizawa, Improvement of soft magnetic properties in (Fe0.85B0.15) 100-xCux melt-spun alloys, Mater. Trans. 48 (2007) 2378–2380.
[8] M. Ohta, Y. Yoshizawa, Magnetic properties of high-Bs Fe–Cu–Si–B nanocrystalline soft magnetic alloys, J. Magn. Magn. Mater. 320 (2008) e750–e753.
[9] M. Ohta, Y. Yoshizawa, High Bs nanocrystalline Fe84-x-yCuxNbySi4B12 alloys (x = 0.0–1.4, y = 0.0–2.5), J. Magn. Magn. Mater. 321 (2009) 2220–2224.
[10] A. Makino, T. Hatanai, A. Inoue, T. Masumoto, Nanocrystalline soft magnetic Fe-M-B (M = Zr, Hf, Nb) alloys anf their applications, Mater. Sci. Eng. A226–228 (1997) 594–602.
[11] M.A. Willard, D.E. Laughlin, M.E. McHenry, D. Thoma, K. Sickafus, J.O. Cross, V.G. Harris, Structure and magnetic properties of (Fe0.5Co0.5)88Zr7B4Cu1 nanocrystalline alloys, J. Appl. Phys. 84 (1998) 6773–6777.
[12] M.A. Willard, M.Q. Huang, D.E. Laughlin, M.E. McHenry, J.O. Cross, V.G. Harris, C. Franchetti, Magnetic properties of HITPERM (Fe, Co)88Zr7B4Cu1 magnets, J. Appl. Phys. 85 (1999) 4421–4423.
[13] A. Makino, H. Men, K. Yubuta, T. Kubota, Soft magnetic FeSiBPCu heteroamorphous alloys with high Fe content, J. Appl. Phys. 105 (2009) 013922.
[14] X.D. Fan, H. Men, A.B. Ma, B.L. Shen, Soft magnetic properties in Fe84-xB10C6Cux nanocrystalline alloys, J. Magn. Magn. Mater. 326 (2013) 22–27.
[15] X. Fan, A. Ma, H. Men, G. Xie, B. Shen, A. Makino, A. Inoue, Fe-based nanocrystalline FeBCCu soft magnetic alloys with high magnetic flux density, J. Appl. Phys. 109 (2011) 07A314.
[16] V. Cremaschi, G. Sánchez, H. Sirkin, Magnetic properties and structural evolution of FINEMET alloys with Ge addition, Physica B 354 (2004) 213–216.
[17] A. Makino, T. Bitoh, A. Inoue, T. Masumoto, Nb-Poor Fe–Nb–B nanocrystalline soft magnetic alloys with small amount of P and Cu prepared by melt-spinning in air, Scr. Mater. 48 (2003) 869–874.
[18] M.E. McHenry, F. Johnson, H. Okumura, T. Ohkubo, V.R.V. Ramanan, D.E. Laughlin, The kinetics of nanocrystallization and microstructural observations in FINEMET, NANOPERM and HITPERM nanocomposite magnetic materials, Scr. Mater. 48 (2003) 881–887.
[19] Y. Yoshizawa, K. Yamauchi, T. Yamane, H. Sugihara, Common mode choke cores using the new Fe-based alloys composed of ultrafine grain structure, J. Appl. Phys. 64 (1988) 6047–6049.
[20] A.K. Panda, B. Ravikumar, S. Basu, A. Mitra, Crystallization and soft magnetic properties of rapidly solidified Fe73.5Nb3Cu1Si22.5 − xBx(x = 5, 9, 10, 11.25, 19) alloys, J. Magn. Magn. Mater. 260 (2003) 70–77.
[21] K. Hono, D.H. Ping, M. Ohnuma, H. Onodera, Cu Clustering and Si Partitioning in the early crystallizaiton stage of an Fe73.5Si13.5B9Nb3Cu1 amorphous alloy, Acta

Metall. 47 (1999) 997–1006.
[22] C. Kuhrt, L. Schultz, Formation and magnetic properties of nanocrystalline mechanically alloyed Fe-Co and Fe-Ni, J. Appl. Phys. 73 (1993) 6588–6590.
[23] M.A. Willard, M. Daniil, K.E. Kniping, Nanocrystalline soft magnetic materials at high temperatures: a perspective, Scr. Mater. 67 (2012) 554–559.
[24] R. Xiang, S. Zhou, B. Dong, G. Zhang, Z. Li, Y. Wang, C. Chang, Effect of Co addition on crystallization and magnetic properties of FeSiBPCu alloy, Progr. Nat. Sci. 24 (2014) 649–654.
[25] Y. Zhang, P. Sharma, A. Makino, Effects of cobalt addition in nanocrystalline Fe83.3Si4B8P4Cu0.7 soft magnetic alloy, IEEE Trans. Magn. 50 (2014) 1–4.
[26] G. Herzer, Grain Size Dependence of coercivity and magnetic conductivity in nanocrystalline ferromagnets, IEEE Trans. Magn. 26 (1990) 1397–1402.
[27] G. Herzer, Modern soft magnets: amorphous and nanocrystalline materials, Acta Mater. 61 (2013) 718–734.
[28] R.K. Roy, A.K. Panda, A. Mitra, Effect of Co content on structure and magnetic behaviors of high induction Fe-based amorphous alloys, J. Magn. Magn. Mater. 418 (2016) 236–241.
[29] Y. Zhang, P. Sharma, A. Makino, Effects of minor precipitation of large size crystals on magnetic properties of Fe-Co-Si-B-P-Cu alloy, J. Alloys Compd. 709 (2017) 663–667.
[30] F. Wang, et al., Soft magnetic Fe-Co-based amorphous alloys with extremely high saturation magnetization exceeding 1.9 T and low coercivity of 2 A/m, J. Alloys Compd. 723 (2017) 376–384.
[31] F. Wang, A. Inoue, Y. Han, F.L. Kong, S.L. Zhu, E. Shalaan, F. Al-Marzouki, A. Obaid, Excellent soft magnetic Fe-Co-B-based amorphous alloys with extremely high saturation magnetization above 1.85 T and low coercivity below 3 A/m, J. Alloys Compd. 711 (2017) 132–142.
[32] Y. Han, J. Ding, F.L. Kong, A. Inoue, S.L. Zhu, Z. Wang, E. Shalaan, F. Al-Marzouki, FeCo-based soft magnetic alloys with high Bs approaching 1.75 T and good bending ductility, J. Alloys Compd. 691 (2017) 364–368.
[33] Y. Zhang, P. Sharma, A. Makino, Effects of cobalt addition in nanocrystalline Fe83.3Si4B8P4Cu0.7soft magnetic alloy, IEEE Trans. Magn. 50 (2014) 2003004.
[34] C. Miguel, A. Zhukov, J.J. del Val, J. González, Coercivity and induced magnetic anisotropy by stress and/or field annealing in Fe- and Co- based (Finemet-type) amorphous alloys, J. Magn. Magn. Mater. 294 (2005) 245–251.
[35] M. Kuhnt, X. Xu, M. Amalraj, P. Kozikowski, K.G. Pradeep, T. Ohkubo, M. Marsilius, Th. Strache, Ch. Polak, M. Ohnuma, K. Hono, G. Herzer, The effect of Co addition on magnetic and structural properties of nanocrystalline (Fe, Co)-Si-B-P-Cu alloys, J. Alloys Compd. 766 (2018) 686–693.
[36] L. Jiang, Y. Zhang, X. Tong, T. Suzuki, A. Makino, Unique influence of heating rate on the magnetic softness of Fe81.5Si0.5B4.5P11Cu0.5C2 nanocrystalline alloy, J. Magn. Magn. Mater. 471 (2019) 148–152.